J Incl Phenom Macrocycl Chem
DOI 10.1007/s10847-016-0688-y

ORIGINAL ARTICLE

Characterization, drug release profile and cytotoxicity of Dentatin-Hydroxypropyl-β-Cyclodextrin complex

Al-Abboodi Shakir Ashwaq[1] · Abdullah Rasedee[2] · Ahmad Bustamam Abdul[1,3] · Yun Hin. Taufiq-Yap[4] · Mothanna Sadiq Al-Qubaisi[1] · Eltayeb E. M. Eid[5]

Received: 19 August 2016 / Accepted: 19 December 2016

Abstract This current work has been conducted mainly to increase solubility and drug release properties for high hydrophobic Dentatin (DEN) by incorporation it into Hydroxypropyl-β-Cyclodextrin (HPβCD) cavity. To confirm that inclusion be succeeded, the produced complex were installed onto different machines. The latter includes: Fourier transform infrared spectroscopy (FT-IR), X-ray diffractometry (XRD), differential scanning calorimetry (DSC), and field emission-scanning electron microscopy (FE-SEM). The hydrodynamic diameter and zeta potential of DEN-HPβCD complex were 2.025 ± 0.39 nm and −33.6 mV, respectively. Ultra-violet spectroscopy was employed to further confirmation of complexation process as well as to determine drug release profile. The result showed an initial burst release (19.9% within first two minutes) and then a continuous release for an extended period of 41 h (100%). The solubility of DEN was enhanced by >300 fold following complexation when a compared to DEN alone. Moreover, MTT finding showed that this complexation did not reduce cytotoxicity of DEN after applying on prostate cancer (LNCaP), human adenocarcinoma breast cancer (MDA-MB-231) and human gastric adenocarcinoma cell line (HDT). However, further investigations are required to validate efficacy of our produced inclusion using molecular analysis and in vivo studies.

Keywords Dentatin · Hydroxypropyl-β-cyclodextrin · Physical properties · Solubility · Drug release

✉ Al-Abboodi Shakir Ashwaq
ashwaq.shaker@yahoo.com

1 Institute of Bioscience, University Putra Malaysia, 43400 UPM Serdang, Selangor, Malaysia

2 Faculty of Veterinary Medicine, Universiti Putra Malaysia, 43400 UPM Serdang, Selangor, Malaysia

3 Department of Biomedical Science, Faculty of Medicine & Health Science, University Putra Malaysia, 43400 UPM Serdang, Selangor, Malaysia

4 Department of Chemistry, Faculty of Science, University Putra Malaysia, 43400 Serdang, Selangor, Malaysia

5 Uniazah College of Pharmacy, Qassim University, Buraydah, Saudi Arabia

Introduction

Nanoparticle technology is used to improve to bioavailability of compounds, particularly after oral administration [1]. Nanoparticles are used to modify the solubility properties of hydrophobic compounds for delivery to tissues [2].

Recently several studies were conducted to determine the potential of hydroxypropyl-β-cyclodextrin (HPβCD), a cyclic oligosaccharide, to be developed as a carrier for therapeutic compounds. The HPβCD has a hydrophobic inner cavity and a hydrophilic external surface with diameter of 6.0 to 6.5 Å [3, 4]. This cyclic oligosaccharide is prepared by modifying β-cyclodextrin (β-CD) to include a hydroxyl propyl group using a base solubilised solution of β-CD with propylene oxide as treatment. The addition of the hydroxyl propyl group to β-CD had its solubility by more than 27 folds [5–7]. In clinical trials showed that HPβCD is safe and tolerated by subjects without the side-effects of β-CD [8]. The solubility characteristics of HPβCD can be benefitted to increase solubility for lipophilic active compounds and improve their bioavailability, while reducing toxicity and prolonging shelf-life [9–13]. Encapsulating a sufficient amount of the certain compound is one of the most wanted properties for cyclodextrin usage [14]. The HPβCD encapsulate a hydrophobic compound within an

lipophilic aqueous component, while liposomes also entrap the hydrophilic drug within the outer layer [15, 16].

Modern therapeutic compounds are challenged by their drug resistance and side-effects. As an alternative, researches are not geared to the discovery of products from plants with medicine values. One such plant is the wild shrub *Clausena excavata* Burm. F [17]. This plant family has approximately 150 genera and 1500 species largely distributed in tropical and subtropical parts of the world that include the Himalayas, Malaysia, China, Indonesia, Thailand and Southeast Asia [18]. The are many products from *C. excavata* with therapeutic properties, among them is the coumarin, Dentatin (5-methoxyl-2,2-dimethyl-10-(1,1-dimethyl-2-propenyl) dipyran-2-one) (DEN) that can be isolate from the roots of the plant with a molecular mass of 326.386 Dalton [19]. This compound was shown to be toxic to various cancer cell lines including prostate, liver, and colon cell lines by modulating the anti-apoptotic molecules Bcl-xL, Bcl-2, and Survivin expressions, inhibition of NF-κB nuclear translocation and the activation of mitochondrial-dependent caspase cascade [20, 21]. The solubility of DEN in water is very poor which leads to complications to its application in dosage forms.

In pharmaceutical science, maintenance the therapeutic window in the body system for a biologically active compound is difficult endeavour because the body in its defense attempts to clear compound that are potentially toxic quickly. One the best method of increasing efficacy of a drug is incorporate into a system that allows for sustained release [22]. In the form of sustained released composition, the concentration of the drug can be maintained at a constant drug concentration for a long period. This can be achieved via the nanoparticle carrier systems. There are several nanoparticle carrier systems being investigate for and some already commercialised for therapeutic use. The nanostructured therapeutic compounds commercially available are nanocrystalline drugs e.g. Rapamune® and Emend®, liposomes e.g. Doxil® and Caelyx®, poly-drug conjugates e.g. Adegen® and Onscapar®, the polymeric micelles, Genoxol-PM®, protein nanoparticles Abraxane®, and the lipid colloid dispersion, Amphotec®.

The formulation of DEN-loaded HPβCD inclusion complex (DEN-HPβCD) is a first to be developed for the delivery of DEN. In this study, the DEN-HPβCD prepared and characterized to determine its physicochemical properties.

Methodology

Materials

Clausena excavata Burm. F. used in this study was obtained from Pendang, Kedah, Malaysia, in December 2014. Dr Shamsul Khamis (Resident Botanist), a member of the Biodiversity Unit, Institute of Bioscience, University Putra Malaysia identified the plant. The plant materials were air-dried and broken into fragments and finally ground to powder. HPβCD (purity ≥ 98%) used in this experiment was purchased from Sigma Aldrich. Trypsin, phosphate-buffered saline (PBS), dimethyl sulfoxide (DMSO), Dulbecco's modified Eagle's medium (DMEM), 3-(4,5-dimethylthiazol-2-yl)-2,5 diphenyltetrazolium bromide (MTT), and trypan blue dye were bought from Sigma Chemical Company (St. Louis, MO, USA). All the chemical materials and reagents used were of analytical grade. Throughout the experimental steps, ultrapure water was used.

Extraction and identification compound

Clausena excavata roots were extracted at room temperature (25–27 °C) by employing organic solvent. Chloroform was used to extract the coarse *C. excavate* root powder (1432 g), which was kept in two 5 L flasks for three days and then filtered. Rotary evaporation was used to concentrate the extracts at 45–50 °C under reduced pressure. The extracts were completely dried to yield crude extracts. A column chromatography over silica gel stepwise gradient elution system was employed to obtain fractions of the extracts. Through these extracts, DEN was isolated from second fraction in the form of white needle-shaped crystals and then characterised by nuclear magnetic resonance (NMR), electron impact mass spectra (EI-MS) [21] .

Phase solubility study

Solubility study was done according to the by Higuchi and Connors 1965 [23]. An excess of DEN was added to ethanol and slowly mixed with 10 mL ultrapure water containing several concentration of HPβCD (0, 2, 4, 6, 8, and 10 mM). The suspensions were then continuously stirred for 72 h at 25 °C until dissolution equilibrium comes into view (clear solution). The samples were then filtered through 0.45 µm nylon filters (waters, USA). The concentration of DEN in the mixture was determined spectrophotometrically at λ of 288.6 nm. The apparent stability constants, K, were derived from the phase solubility diagram using the equation: $K = Slope/S_0$ (1-slope), where S_0 is the intrinsic solubility of the drug in water.

Preparation of the inclusion complex

The DEN-HPβCD complex (DEN-HPβCD) was prepared using the freeze-drying method. This requires preparing DEN solutions in HPβCD at 1:1 molar ratio; 0.3264 g DEN was dissolved in 5 mL chloroform, which was mixed with 1.4 g HPβCD in 20 mL of ultra-pure water. The mixture

was stirred at room temperature for 72 h and then filtered using 0.45 µm filter paper. The resultant clear solution was frozen at −80 °C, which was subsequently freeze-dried for 24 h at −55 °C.

Drug loading

The loading amount of DEN in the complex was determined using a Perkin-Elmer Lambda 35 UV-visible spectrophotometer. A known weight of complex (1.2614 mg) was placed in a 10 mL volumetric flask, and 0.5 mL of 1 mol/L HCl solution was added. The concentration of DEN in the solution was determined at 0.236445 mg/ml using the standard curve of a series of standard solutions of known DEN concentrations. The drug load and encapsulation efficiency were calculated by Equations (1) and (2), respectively.

$$\text{Drug loading} = A/B \times 100 \quad (1)$$

$$\text{Encapsulation efficiency} = (C - D)/C \quad (2)$$

where A is the weight of drug (DEN) in the complex, B is the gross weight of complex, C is the total weight of drug, and D is the weight of drug (DEN) that remained in the liquid medium after encapsulation. A parallel to that, standard for DEN vs Absorbance was drawn.

Characterisation

The potassium bromide (KBr) disc technique was used to examine the FT-IR spectra of compounds and the technique was performed using FT-IR spectra 100 (Perkin-Elmer, USA). A scanning range of 4000 to 250 cm^{-1} at an ambient temperature was chosen to determine the FTIR measurements. X-Ray diffractometer (Panalytical X, Pert Pro MPD) model was chosen to perform Powder XRD analysis, which used CuKα radiation, λ 1.5406 A^0. Differential scanning calorimetric analyses (DSC) were carried out at a temperature range of 25–200 °C with a heating rate of 10 °C/min under a nitrogen atmosphere (N_2 flow rate 50 mL/min) on a Mettler Toledo instrument (Switzerland). The surface morphology of the samples was examined using a field emission scanning electron microscope (FESEM, JSM-7600F, JOEL, Japan). A Zeta Sizer Nano ZS (Malvern Instruments Ltd, Malvern, UK) with dynamic light scattering was used to measure the hydrodynamic size and zeta potential of DEN-HPβCD dispersion (1 µg of DEN-HPβCD complex dissolved in 1 mL of ultra-deionized water). UV- Vis spectra were recorded with Perkin-Elmer Lambda 35 UV-visible spectrophotometer. The UV-Vis absorption spectra of the DEN, HPβCD and DEN- HPβCD complex were recorded against a reagent blank (ethanol) prepared with the same reagent concentration.

Release Study of DEN from DEN-HPβCD inclusion complex

Release of DEN from the DEN-HPβCD inclusion was determined. The DEN-HPβCD (85 g) was place in 250 mL phosphate-buffered solution of pH 7.4. The amount of DEN released into surrounding solution was determined using the UV-visible spectrophotometer at 388.1 nm (model Lambda 35; Perkin-Elmer). The absorbance was readed every one minute up to 4500 min. The increasing in absorbance is proportional to the dissociated quantity of DEN.

Cell line and cell culture

Human gastric adenocarcinoma cell line (HDT) and human adenocarcinoma breast cancer cells (MDA-MB-231) and the normal human breast (MCF-10a) cells obtained from American Type Culture Collection were maintained in Dulbecco's Modified Eagles medium (DMEM).The Roswell Park Memorial Institute medium 1640 (RPMI 1640) was used to grow the human prostate cancer (LNCaP) cells. Both media were supplemented with 10% foetal bovine serum, 1% amphotericin B and 1% penicillin–streptomycin. The cells were maintained in a humidified incubator maintained at 37 °C and under 5% CO_2 and examined frequently under an inverted microscope (Micros, Austria).

Cytotoxicity assay

The 3-(4,5-dimethylthiazol-2-yl)-2,5-diphenyltetrazolium bromide (MTT) assay was employed to determine the effect of DEN and DEN-HPβCD on the cancer cells. Cells seeded in a flask were washed twice with 2 mL phosphate-buffered saline (PBS) and incubated with 1 mL of trypsin in 37 °C under 5% CO_2 for 5 min to detach. Five millilitres of DMEM were then added to the flask and the cells stained with trypan blue and enumerated using a haemocytometer.

Both DEN and DEN-HPβCD complex solutions was dissolved in culture media serially to concentrations of 1.56, 3.125, 6.25, 12.5, 25, 50, and 100 µg/mL. One hundred microliters of 1×10^5 cells/mL of each cancer cell line was added to the assigned wells of a 96-well culture plate. Control wells contained cell-free DMEM solution with or RPMI 1640 and untreated cells. The plate was incubated in 37 °C under 5% CO_2 for 24 h before the medium was removed and 100 µL each of DEN and DEN-HPβCD complex solution at various concentrations added to the respective wells. The plate was incubated for another 72 h at 37 °C under 5% CO_2. At the end of the treatment period, the medium was removed and the wells replenished with fresh medium and 20 µL of 5 mg/mL MTT solution added. The plate was again incubated at a temperature of 37 °C under

5% CO_2 for 4 h, the medium discarded and replaced with 100 µL of DMSO to dissolve the formed formazan crystals. The experiment was done in triplicates. The culture plates were shaken for 5 min and read in an ELISA reader (model, manufacturer) to determine the absorbance (OD) at 570 with reference wavelength of 630 nm. The anti-proliferative activities of the treatment compounds were determined as follows:

$$\text{Cell viability (\%)} = \frac{OD_{Sample} - OD_{Blank}}{OD_{Control} - OD_{Blank}} \times 100$$

where OD_{Sample} is the absorbance of the sample, OD_{Blank} is the absorbance of the blank, and $OD_{Control}$ is the absorbance of the control.

Results and discussion

Compound isolation and identification

The EI-MS and ^1H NMR results are consistent with those reported earlier by (Nakamura et al. 2009) [24] and (Songsiang et al. 2012) [25]. The EI-MS analysis indicated the presence of molecular ion peak at m/z (326), which corresponds to the molecular formula of DEN ($C_{20}H_{22}O_4$) (Fig. 1). As depicted in (Fig. 2a), the spectral data of ^1H ($CDCL_3$, 500 MH_Z, *CHLOROFORM-d*) were δ ppm: 1.46 (s, 6 H), 1.67 (s, 6 H), 3.84 (s, 3 H), 4.89 (d, $J = 9.78$ Hz, 1 H), 4.95 (d, $J = 16.63$ Hz, 1 H), 5.71 (d, $J = 9.78$ Hz, 1 H), 6.20 (d, $J = 9.54$ Hz, 1 H), 6.31 (dd, $J = 17.36$, 10.52 Hz, 1 H), 6.58 (d, $J = 10.03$ Hz, 1 H), 7.88 (d, $J = 9.54$ Hz, 1 H); (Fig. 2b) showed that the C-NMR ($CDCL_3$, 150 MH_Z) were δ: 27.5 (C-5′ C-6′), 29.4 (C-4″, C-5″), 41.1 (C-1″), 63.4 (OCH_3), 77.4 (C-2′), 107.5 (C-10), 108.2 (C-3″), 108.4 (C-3), 111.7 (C-6), 116.3 (C-4′), 119.2 (C-8), 130.3 (C-3′), 138.9 (C-4), 149.8 (C-2″), 151.2 (C-9), 153.9 (C-5), 156.0 (C-7), 160.7 (C-2).

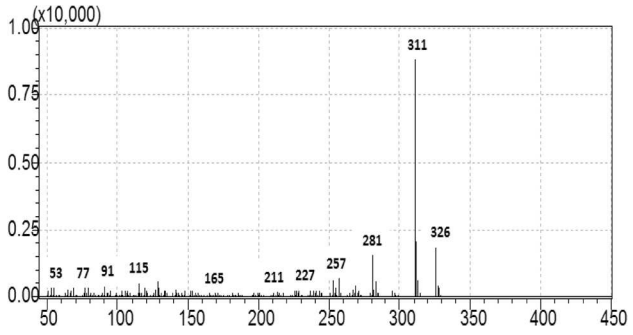

Fig. 1 Electron impact mass spectrum (EI-MS) of dentatin, X-axis represent mass over charge (m/z). Y-axis represent relative intensity. The last peak (326) was represented molecular weight of dentatin and the long peak represented base peak (molecular weight of dentatin without CH3 group)

Phase solubility analysis

The phase solubility diagram for DEN and HPβCD obtained based on the methods of Higuchi and Connors 1965 (Fig. 3) can be categorised as AL-type. The solubility of DEN increases linearly with increase HPβCD concentration. The stability constant K was obtain from the linear portion in the phase solubility diagram described by the following formula.

$$K = \text{slope}/S_0(1 - \text{slope})$$

where S_0 represents the intrinsic solubility of DEN when HPβCD is not present in the solution. (Table 1) shows the value of the stability constant K from the phase solubility assay. Determination of stability constant K is useful because it reveals rate of drug dissociation from capsule to surrounding media. This was found to be the best suited to enhance the drug solubility and stability, which enables its controlled release from the inclusion complexes [26]. The phase solubility analysis showed that DEN-HPβCD complex increases stability and solubility of DEN. The aqueous solubility of DEN was 0.035 mM that increased to 10.99 mM when in complexation with HPβCD showing that water solubility of DEN had increased by more than 300 times. The ability of HPβCD to improve solubility of compounds was also previous shown when β-Lapachone was incorporated in a complex with the carrier [27]. Nevertheless, the reliability of the obtained satisfactory solubility of the DEN-HPβCD complex is proven by these results. This will be beneficial for the medical application of DEN.

Drug load and encapsulation efficiency

Drug load and encapsulation efficiency are parameters that determines the suitability of a compound to be used as a drug carrier. In this study, drug-loading and encapsulation efficiency of DEN in HPβCD was 18.7 and 99.1%, respectively, which is better that loading of most alkaloids [28].

Fourier transform infrared spectroscopy

The FT-IR spectroscopy is a method to show complex formation of a guest molecule with a carrier. The FT-IR spectra of DEN, HPβCD, physical mixture and DEN-HPβCD complex are shown in Fig. 4. A band is present at 2968, 3007 cm^{-1}, which shows that there is C–H stretching of the aromatic ring. A strong band at 1722 cm^{-1} can also be seen that corresponds to the C=O of the carbonyl group. C=C aromatic group is presented by the band at 1586 cm^{-1}.

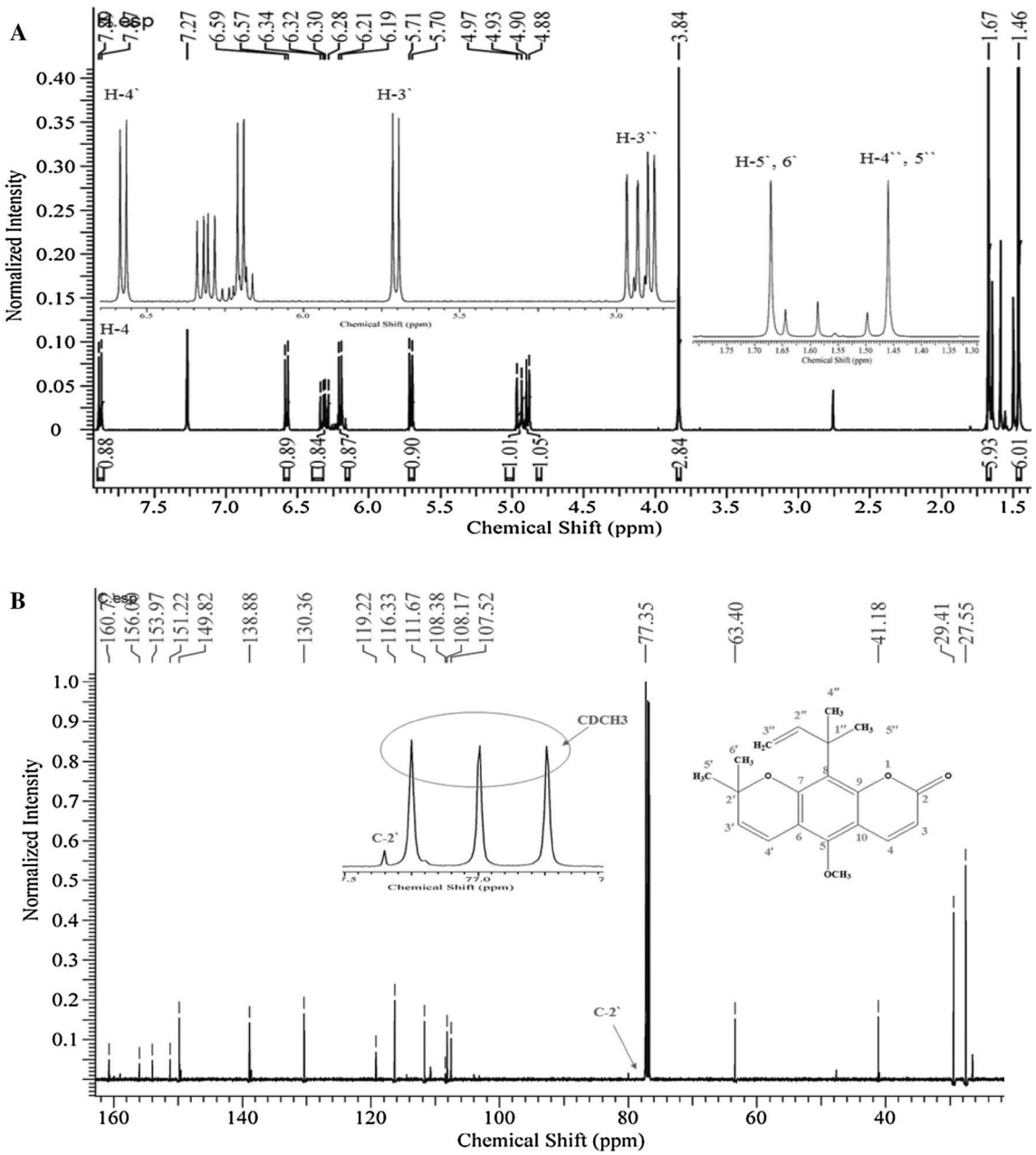

Fig. 2 **a** Proton nuclear magnetic resonance (1H-NMR) Spectrum of 5-methoxy-2′,2′-dimethyl 10-(1,1-dimethyl-2-propenyl) dipyran-2-one (Dentatin), each peak represent one type of protons (integration) exist in the sample with specific chemical shift **b** Carbone-13 nuclear magnetic resonance (^{13}C-NMR) Spectrum of 5-methoxy-2,2′dimethyl-10-(1,1-dimethyl-2-propenyl) dipyran-2-one (Dentatin), the number of carbone atoms exist in sample was represented as peaks appeared with specific chemical shift

The peaks in the range of 1323–1460 cm^{-1} represents the alkane (–C–H) groups. Ester groups and ether group ranges are represented by the peaks in the range of 1084 to 1282 cm^{-1}. The peaks in the range of 713–970 cm^{-1} represent the alkene (=C–H) groups. (Fig. 4b–d) represent the FTIR spectra of HPβCD, physical mixture and DEN-HPβCD, respectively. However, after the inclusion complex was formed, considerable changes in the FT-IR spectra were discovered. In the inclusion complex (Fig. 4d), most bands in DEN were not seen. This observed changes in the FT-IR spectra of DEN combined with HPβCD due to the restriction of the vibration of DEN molecule after encapsulation into the HPβCD cavity. At the same time, many peaks in the HPβCD were shifted slightly and enhanced its intensity in DEN-HPβCD inclusion complex spectra. In addition, an extra peak at 1725 cm^{-1} was seen in DEN-HPβCD complex spectra which belonging to the carbonyl group of DEN. These results indicate that the DEN-HPβCD

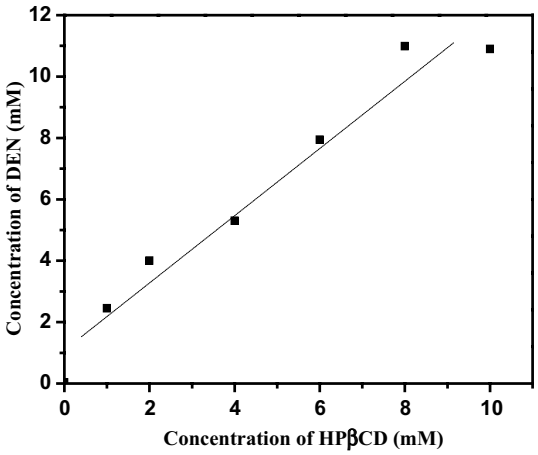

Fig. 3 Phase solubility of DEN- HPβCD. We can see the increasing of HPβCD concentration enhanced solubility of DEN in proportional way

Table 1 Intrinsic solubility of DEN (S_0) and stability constant (K) values calculated from the linear portion in the phase solubility diagram

DEN-HPβCD	S0 (mM)	Slope	R2	K (mM^{-1})
	0.035	0.9775	0.9582	1243.42

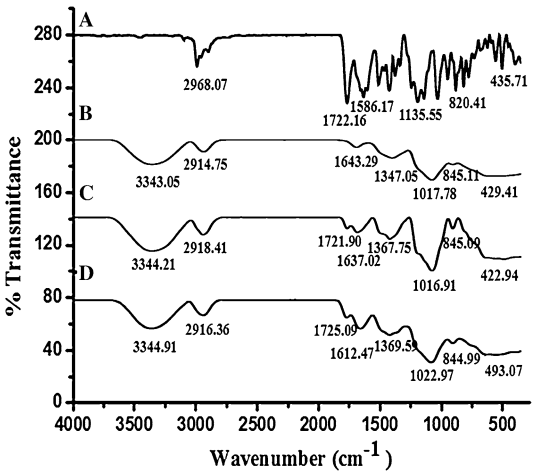

Fig. 4 Fourier transform infrared spectrum for **a** dentatin (DEN), **b** HPβCD, **c** physical mixture and **d** DEN-HPβCD complex. It can be noticed easily the absence of most functional groups of DEN following incorporation to HPβCD cavity which in turn approved the successful inclusion

complex changed the typical DEN spectrum to the most complex one, indicating a complete integration of compound in the DEN-HPβCD complex [29–32]

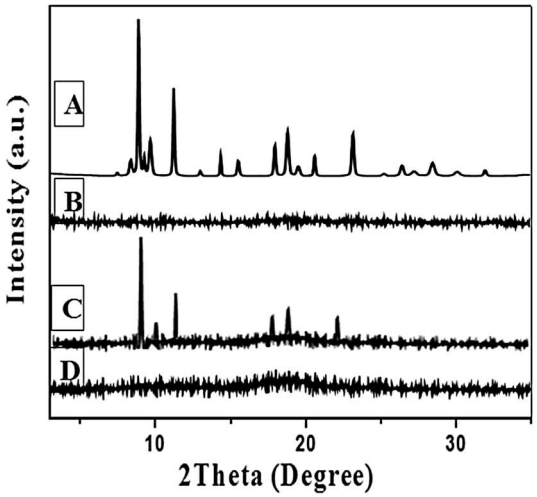

Fig. 5 X-ray diffractogram patterns for **a** dentatin (DEN), **b** HPβCD, **c** physical mixture and **d** DEN-HPβCD complex. It can be noticed easily the absence of all peak of DEN crystal following incorporation to HPβCD cavity to produced amorphous phase for produced complex which in turn approved the successful inclusion

X-ray diffraction

A useful method to detect the complexes in crystalline and amorphous states is by X-ray diffraction (XRD) analysis [33]. Hence, the complexation between DEN and HPβCD was further investigated by XRD. The XRD patterns for DEN, HPβCD, physical mixture and DEN-HPβCD complex are shown in (Fig. 5). Various high-intensity sharp peaks were revealed by XRD patterns of DEN at several diffraction angles (2θ) of 9.05°, 11.42°, 14.42°, 15.51°, 18.84°, 19.60°, 23.24°, 25.27°, 27.30° and 30.07°, which are evidences that the DEN is crystalline (Fig. 5a). The same diffraction peaks clearly appeared in the physical mixture which indicate to absence the interaction between DEN and HPβCD (Fig. 5c). On the other hand, apart from two broad halos, HPβCD pattern did not show any sharp peak. This shows that the HPβCD is amorphous (Fig. 5b). The DEN- HPβCD no longer exhibit the typical peaks where all the diffraction peaks of DEN were completely vanished. Lack of crystallinity is evidence to happened complexation between DEN and HPβCD. Furthermore, this behaviour leads to the formation a new solid phase which represented by converted the crystalline phase to amorphous phase. However, The study shows that DEN in complex with HPβCD was not crystalline but instead adopted the amorphous nature of the carrier [34, 35]. The same findings has been reported by (Eid et al., 2011) [36], when used HPβCD to prepare complex with zerumbone.

Thermal analysis

Thermal analytical techniques including differential scanning calorimetric (DSC) are used to determine the physical state of the molecules and compounds [37]. Incorporation of molecules into a carrier changes their boiling, sublimation, and melting points to various temperatures within temperature range HPβCD decomposition [38, 39]. The DSC pattern for DEN shows a sharp endothermic peak at 85.6 °C, which is its melting point (Fig. 6a). The DSC thermogram of the HPβCD shows a broad endothermic peak 100 °C that are corresponds with loss of water molecule at that temperature (Fig. 6b). On the other hand, the DSC pattern of DEN was observed in the physical mixture, but with marked reduction of less intensity. This marked changes attributed to the fusion between DEN melting and HPβCD decomposition which due to interaction of the vicinity of the two effects. Furthermore, the marked reduction in intensity of the melting peak aforementioned result is a clear single of the low DEN to HPβCD molar ratio (1:1). In addition, the obvious existence of DEN melting peak in the physical mixture is proved evidence that no true inclusion complex was formed between DEN and HPβCD (Fig. 6c). In the DEN-HPβCD pattern, the endothermic peak occurs at 78.98 °C. The analysis shows the melting point of DEN-HPβCD is not the same with either of DEN, HPβCD or physical mixture. As can be seen from (Fig. 6d), the melting peak of DEN was vanished completely, this evidence to the molecular encapsulation of DEN in to the HPβCD cavity. However, The DEN- HPβCD is amorphous in nature unlike the crystalline pure DEN [40].

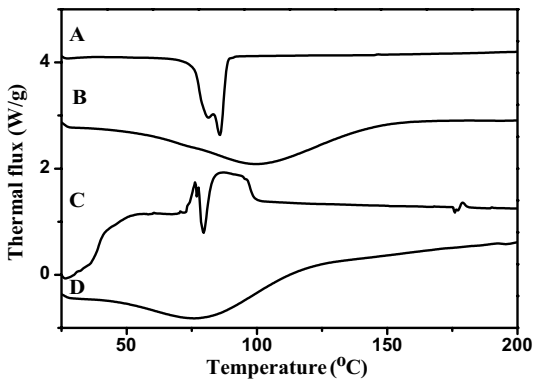

Fig. 6 Differential scanning calorimetric pattern for **a** DEN, **b** HPβCD, **c** physical mixture and **d** DEN-HPβCD complex. The shifting of melting point from 85.6 °C for free DEN to 78.98 °C after encapsulation demonstrated the elevation in thermostability of DEN as a result of incorporation

Filed emission scanning electron microscopy (FE-SEM)

The surface morphology of DEN, HPβCD, physical mixture and DEN-HPβCD complex were analysed using the FESEM technique. FESEM images analysis of all the samples are depicted in (Fig. 7). Pure DEN forms a crystalline structure of various sizes. HPβCD appears to be porous, spherical with cavities. The scanning electron microscopy of physical mixture showed same surface morphology of ingredients when scanning them separately, Both the characteristic crystals of DEN and spherical particles of HPβCD were clearly observed in the physical mixture, this indicate there is no complexation occurred between DEN and HPβCD. In addition, the specific morphology of HPβCD which represented with porous and spherical shape disappeared as a result of complex formation with DEN. However, the DEN-HPβCD complex exhibited irregularly amorphous pieces with various dimensions, which were relatively different from the shapes and sizes of DEN and HPβCD particles. These analyses confirmed the existence of new solid phase that are due to the formation of the inclusion complex [41, 42].

Size and zeta potential

The particle diameter was found to be 2.025 ± 0.39 nm as shown in (Fig. 8a), while the zeta potential for the DEN-HPβCD complex suspensions was −33.6 Mv (Fig. 8b). Besides the biomolecular approach, it is well known that surface charge, shape, and size are the primary parameters of colloidal particles for cellular uptake [43]. Size analysis showed that the hydrodynamic diameters of DEN-HPβCD complex were 2.025 nm which approximately form 37% of the total reading, and the another peaks were larger than proposed with average 380.7d.nm and the PDI was 0.616. This may suggest that our complex tends to aggregate in deionized and double-distilled water, and their low zeta potential of −33.6 mV indicates that the formulated complex have poor electrostatic repulsion characteristics and thus are of incipient instability. At this zeta potential (−33.6), the produced complex would not repel particle aggregation in suspensions for long-term stability. Generally, the cells have fewer uptakes of particles with negative charge compared to those with positive charge, which might be attributed to the attractive or repulsive interaction between the negatively charged cell membrane and positively/negatively charged particles [44]. The magnitude of the zeta potential indicates that the low degree of electrostatic repulsion conferred its low stability.

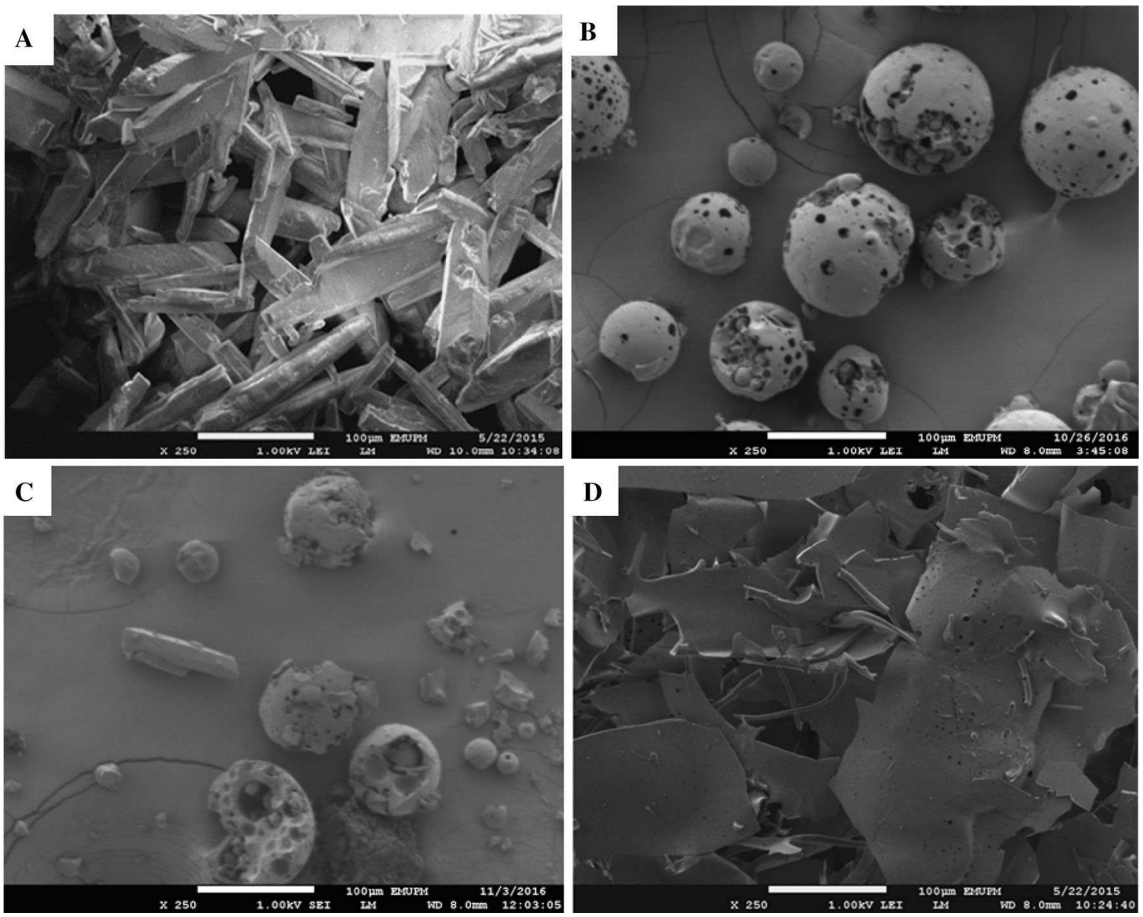

Fig. 7 Field emission scanning electron microscopic image of **a** DEN, **b** HPβCD, **c** physical mixture and **d** DEN-HPβCD complex. The powdered samples were snapped under high magnification (250 X)

Ultraviolet absorbance analysis

The UV-Vis spectra of DEN is presented as a function of HPβCD at 25 °C. The pattern of DEN spectrum changed only slightly upon complexing with HPβCD (Fig. 9). This is consistent with results shown by other studies when oxybenzone was incorporated of into β-CD and albendazole into cyclodextrin. The pattern of the UV-Vis spectrum of molecule alone and those of their complexes did not vary significantly [45]. There was only a small shift to a higher wavelength of the absorbance peak from 288.6 nm of DEN alone to 291.5 nm of the DEN-HPβCD. The wavelength shift is consistent with the intensity of DEN-HPβCD complex than free DEN [46].

Release behaviour of DEN

To investigate the DEN release behavior from the complex, the inclusion were incubated in phosphate buffer pH 7.4 release media and assessed by UV spectra-photometry [47–49]. However, the after initial burst effect, release of DEN from DEN-HPβCD became more gradual (Fig. 10a). All incorporated DEN was released only after more than 40 h of incubation. This study shows that the DEN-HPβCD complex is an excellent form of delivery of DEN for therapeutic effect.

Release kinetics of DEN from the DEN-HPβCD complex

The data of the cumulative release of the DEN from the complex were described by three kinetic models, which are described as follows:

Zero-order model equation:

$$q_t = q_0 + k_0 t \tag{1}$$

where qt is the amount of drug dissolved in time t, q0 is the initial amount of drug in the solution and K0 is the zero order release constant expressed in units of concentration/time.

The results indicated that the release of the DEN from the complex followed the Zero-order.

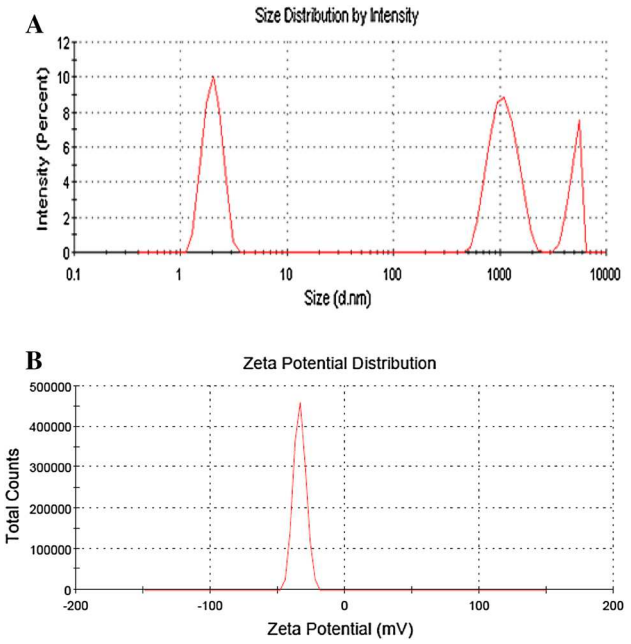

Fig. 8 Particle size (**a**) and Surface charge (**b**) of DEN-HPβCD. Figure A shows wide range in size of suspended particles with narrow ranged surface charge

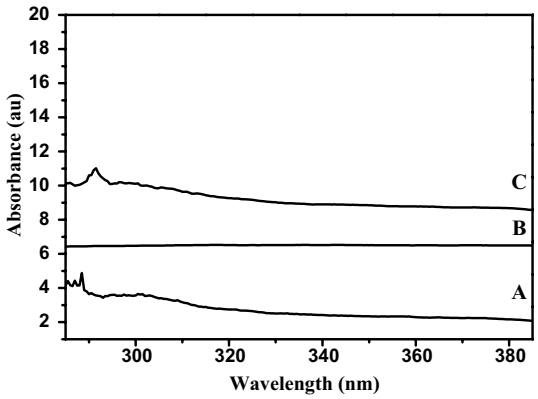

Fig. 9 Ultraviolet–visible absorption spectra of **a** DEN, **b** HPβCD, and **c** DEN-HPβCD Complex. We can see a shifting in the peak of encapsulated drug to the right when a compared to the free drug

Kinetic model, with a best fit value for the correlation coefficient (R^2) at 0.95791, as shown in Table 2 and Fig. (10b).

Cytotoxicity assay

In this study the cytotoxicity activity of both DEN (dissolved in organic solvent DMSO) and DEN-HPβCD complex against human adenocarcinoma breast cancer (MDA-MB-231), prostate cancer (LNCaP) and human gastric adenocarcinoma cell line (HDT) was determined by using

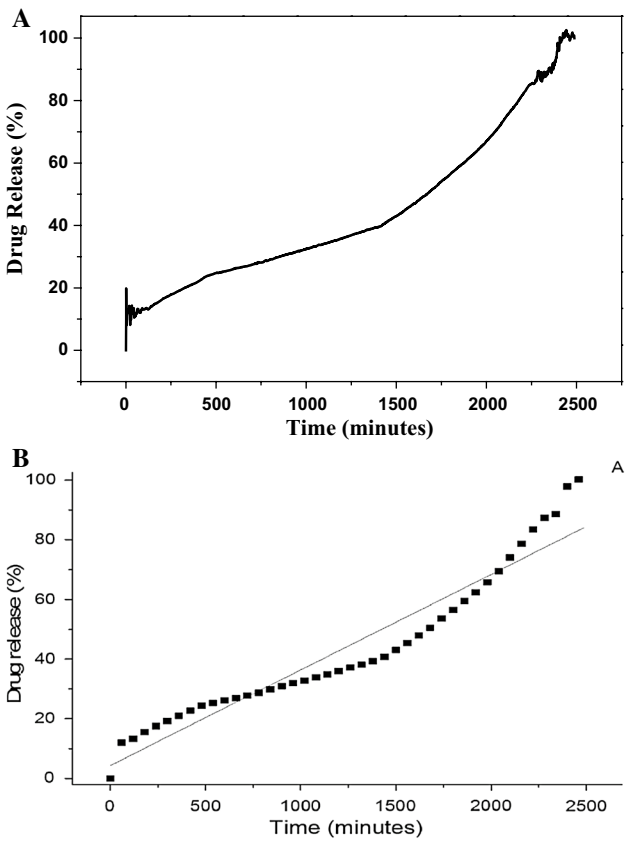

Fig. 10 **a** Release profile of dentatin (DEN) from DEN HPβCD in PBS buffer. The first two minutes exposure led to release 20% of drug (burst effect) due to weak bound of drug with HPβCD. **b** Data fitting for release kinetics of dentatin (DEN) release from DEN HPβCD into PBS buffer solution. The release kinetic model is zero order

Table 2 Zero-order kinetic models with correlation coefficient (R^2) of dentatin (DEN) release from DEN- HPβCD into PBS buffer solution

Model	Equation	R^2	R^2-adj	Sum of squares of residue
Zero-order	Y = 0.03204 * X + 4.31494	0.95791	0.91757	118435.613

MTT assay. The cells were treated with different concentrations (1.5–100 μg/mL) for 72 h. This study showed that DEN and DEN-HPβCD complex have significant cytotoxicity effects against HDT and LNCaP cells at concentrations (100, 50, 25, 12.5, 6.25 and 3.125) ($P < 0.05$) compare with the control. In contrast, there is no significant effects on cells growth at lowest concentration 1.560. In another hand, MDA-MB-231 showed sensitivity for all DEN concentrations. While there is no significant effects at the lowest concentrations (3.125 and 1.560) when treated with DEN-HPβCD complex. The IC_{50} values (concentration causing death of 50% of tested cells) of DEN and

Table 3 IC_{50} values of DEN and DEN-HPβCD complex on MDA-MB-231, HDT, and LNCaP based on MTT assay following exposure for 72 h

Cell line	Dentatin IC_{50} µg/ml	DEN- HPβCD IC_{50} µg/ml
MDA-MB 231	5.68 ± 0.1	7.29 ± 0.3
HDT	7.70 ± 0.8	11.78 ± 0.5
LNCaP	8.51 ± 3.5	12.58 ± 0.6

DEN-HPβCD inclusion complex for the cells are shown in (Table 3). DEN dramatically showed high cytotoxicity effect on all human cancer cells line in a dose- dependent manner. Previous studies carried out by Ismail et al. (2013) showed similar toxicity against Estrogen Receptor positive (ER+) MCF-7 with 6.1 µg/ mL as IC_{50} while DEN has showed 5.58 µg/ mL as IC_{50} against Estrogen Receptor negative (ER-) MDA-MB231 cell line in our current study. According to the mentioned study above, DEN showed less side effect on the (MCF-10 a) normal cells when a compared to cancer cells [50]. In turn, exposure to HPβCD alone didn't exhibit a notable growth inhibitory against normal cells (MCF-10 a) after 72 h.

DEN-HPβCD complex showed a growth inhibition against all treated cells. However, the drug incorporated onto HPβCD cavity exerts less toxicity against all cancer cells than that seen with DEN dissolved in DMSO. These variety in reduction of cells viability between DEN and DEN-HPβCD may be attributable to role DMSO and the time needed for drug release; hence, the gradually release of DEN from complex will prolong the exposure time [51]. Thus, the DEN dissolved in organic solvent exhibited more cytotoxic effect against three cancer cell lines when a compared to DEN incorporated into HPβCD cavity.

Conclusion

Inclusion complex of DEN and HPβCD (1:1) molar ratio was prepared in aqueous solution at room temperature. The resulted DEN-HPβCD complex was characterized by XRD, FT-IR, DSC, FESEM and UV-Vis. All the characterization results appeared that DEN incorporated inside the cavity of the HPβCD. Furthermore, drug release study showed modify profile of drug release which prolong exposure time of compound. According to the above findings, we conclude that successful incorporation between DEN and HPβCD leaded to improve physiochemical properties of DEN such as solubility, stability and bioviability. However, the inclusion complex, with HPβCD as a carrier, is a new drug and compound delivery system that has great potential for application in the biopharmaceutical industry. The DEN-HPβCD complex is a good candidate for the development of a new compound for the treatment of cancers.

Acknowledgements This research was supported by science fund research grant (02-01-04-sf1210), Ministry of science, Technology and innovation, Malaysia. The author (Al-Abboodi Sh Ashwaq) is grateful to University of AL-Qadisiyah, Ministry of Higher Education and Scientific Research, Iraq.

References

1. Merisko-Liversidge, E.M., Liversidge, G.G.: Drug nanoparticles: formulating poorly water-soluble compounds. Toxicol. Pathol. **36**(1), 43–48 (2008)
2. Shaikh, J., Ankola, D., Beniwal, V., Singh, D., Kumar, M.R.: Nanoparticle encapsulation improves oral bioavailability of curcumin by at least 9-fold when compared to curcumin administered with piperine as absorption enhancer. Eur. J. Pharm. Sci. **37**(3), 223–230 (2009)
3. Szejtli, J.: Introduction and general overview of cyclodextrin chemistry. Chem. Rev. **98**(5), 1743–1754 (1998)
4. Loftsson, T., Brewster, M.E.: Pharmaceutical applications of cyclodextrins: basic science and product development. Journal of pharmacy and pharmacology. **62**(11), 1607–1621 (2010)
5. Al-Rawashdeh, N.A., Al-Sadeh, K.S., Al-Bitar, M.-B.: Physicochemical study on microencapsulation of hydroxypropyl-β-cyclodextrin in dermal preparations. Drug Dev Ind Pharm. **36**(6), 688–697 (2010)
6. Harada, A., Hashidzume, A., Takashima, Y.: Cyclodextrin-based supramolecular polymers. In: Supramolecular polymers polymeric betains oligomers. pp. 1–43. Springer, Berlin (2006)
7. Anirudhan, T.S., Nima, J., Divya, P.L.: Synthesis, characterization and in vitro cytotoxicity analysis of a novel cellulose based drug carrier for the controlled delivery of 5-fluorouracil, an anticancer drug. Appl. Surf. Sci. **355**, 64–73 (2015)
8. Domańska, U., Pelczarska, A., Pobudkowska, A.: Effect of 2-hydroxypropyl-β-cyclodextrin on solubility of sparingly soluble drug derivatives of anthranilic acid. International journal of molecular sciences. **12**(4), 2383–2394 (2011)
9. Danciu, C., Soica, C., Oltean, M., Avram, S., Borcan, F., Csanyi, E., Ambrus, R., Zupko, I., Muntean, D., Dehelean, C.A.: Genistein in 1: 1 inclusion complexes with ramified cyclodextrins: Theoretical, physicochemical and biological evaluation. Int. J. Mol. Sci. **15**(2), 1962–1982 (2014)
10. Singh, R., Bharti, N., Madan, J., Hiremath, S.: Characterization of cyclodextrin inclusion complexes—a review. J. Pharm. Sci. Technol. **2**(3), 171–183 (2010).
11. Aiassa, V., Zoppi, A., Albesa, I., Longhi, M.R.: Inclusion complexes of chloramphenicol with β-cyclodextrin and aminoacids as a way to increase drug solubility and modulate ROS production. Carbohydr. Polym. **121**, 320–327 (2015)
12. Mennini, N., Bragagni, M., Maestrelli, F., Mura, P.: Physicochemical characterization in solution and in the solid state of clonazepam complexes with native and chemically-modified cyclodextrins. J. Pharm. Biomed. Anal. **89**, 142–149 (2014)
13. Mazzaferro, S., Bouchemal, K., Gallard, J.-F., Iorga, B.I., Cheron, M., Gueutin, C., Steinmesse, C., Ponchel, G.: Bivalent sequential binding of docetaxel to methyl-β-cyclodextrin. Int. J. Pharm. **416**(1), 171–180 (2011)
14. Davis, M.E.: Design and development of IT-101, a cyclodextrin-containing polymer conjugate of camptothecin. Adv. Drug Deliv. Rev. **61**(13), 1189–1192 (2009)

15. Szente, L., Szejtli, J.: Highly soluble cyclodextrin derivatives: chemistry, properties, and trends in development. Adv. Drug Deliv. Rev. **36**(1), 17–28 (1999)
16. Pose-Vilarnovo, B., Perdomo-Lopez, I., Echezarreta-Lopez, M., Schroth-Pardo, P., Estrada, E., Torres-Labandeira, J.J.: Improvement of water solubility of sulfamethizole through its complexation with β-and hydroxypropyl-β-cyclodextrin: characterization of the interaction in solution and in solid state. Eur. J. Pharm. Sci. **13**(3), 325–331 (2001)
17. Yu, Z., Cui, M., Yan, C., Song, F., Liu, Z., Liu, S.: Investigation of heptakis (2, 6-di-O-methyl)-β-cyclodextrin inclusion complexes with flavonoid glycosides by electrospray ionization mass spectrometry. Rapid Commun Mass Spectrom. **21**(5), 683–690 (2007)
18. Blumenthal, R.D., Lew, W., Reising, A., Soyne, D., Osorio, L., Ying, Z., Goldenberg, D.M.: Anti-oxidant vitamins reduce normal tissue toxicity induced by radio-immunotherapy. Int. J. Cancer. **86**(2), 276–280 (2000)
19. Arbab, I.A., Abdul, A.B., Abdelwahab, S.I.: Clausena excavata Burm. f.(Rutaceae): A review of its traditional uses, pharmacological and phytochemical properties. (2015).
20. Sharif, N.M., Mustahil, N., Noor, N.M., Sukari, M., Rahmani, M., Taufiq-Yap, Y., Ee, G.: Cytotoxic constituents of Clausena excavata. Afr. J. Biotechnol. **10**(72), 16337–16341 (2013)
21. Arbab, I.A., Looi, C.Y., Abdul, A.B., Cheah, F.K., Wong, W.F., Sukari, M.A., Abdullah, R., Mohan, S., Syam, S., Arya, A.: Dentatin induces apoptosis in prostate cancer cells via Bcl-2, Bcl-xL, Survivin downregulation, caspase-9,-3/7 activation, and NF-κB inhibition. Evidence-Based Complementary and Alternative Medicine **2012** (2012).
22. Kumar, M.: Nano and microparticles as controlled drug delivery devices. J. Pharm. Pharm. Sci. **3**(2), 234–258 (2000).
23. Higuchi, T., Connors, A.: Phase-solubility techniques (1965).
24. Songsiang, U., Thongthoom, T., Zeekpudsa, P., Kukongviriyapan, V., Boonyarat, C., Wangboonskul, J., Yenjai, C.: Antioxidant activity and cytotoxicity against cholangiocarcinoma of carbazoles and coumarins from Clausena harmandiana. Science-Asia: **38**, 75–81 (2012)
25. Nakamura, T., Kodama, N., Arai, Y., Kumamoto, T., Higuchi, Y., Chaichantipyuth, C., Ishikawa, T., Ueno, K., Yano, S.: Inhibitory effect of oxycoumarins isolated from the Thai medicinal plant Clausena guillauminii on the inflammation mediators, iNOS, TNF-α, and COX-2 expression in mouse macrophage RAW 264.7. J. Nat. Med. **63**(1), 21–27 (2009)
26. Wang, L., Yan, J., Li, Y., Xu, K., Li, S., Tang, P., Li, H.: The influence of hydroxypropyl-β-cyclodextrin on the solubility, dissolution, cytotoxicity, and binding of riluzole with human serum albumin. J. Pharm. Biomed. Anal. **117**, 453–463 (2016)
27. Zhang, L., Zhu, W., Lin, Q., Han, J., Jiang, L., Zhang, Y.: hydroxypropyl-β-cyclodextrin functionalized calcium carbonate microparticles as a potential carrier for enhancing oral delivery of water-insoluble drugs. Int. J. Nanomed. **10**, 3291 (2015)
28. Swaminathan, S., Pastero, L., Serpe, L., Trotta, F., Vavia, P., Aquilano, D., Trotta, M., Zara, G., Cavalli, R.: Cyclodextrin-based nanosponges encapsulating camptothecin: physicochemical characterization, stability and cytotoxicity. Eur. J. Pharm. Biopharm. **74**(2), 193–201 (2010)
29. Sancho, M.I., Russo, M.G., Moreno, M.S., Gasull, E., Blanco, S.E., Narda, G.E.: Physicochemical Characterization of 2-Hydroxybenzophenone with β-cyclodextrin in Solution and Solid State. J. Phys. Chem. B **119**(18), 5918–5925 (2015)
30. Liu, M., Cao, W., Sun, Y., He, Z.: Preparation, characterization and in vivo evaluation of formulation of repaglinide with hydroxypropyl-β-cyclodextrin. Int. J. Pharm. **477**(1), 159–166 (2014)
31. Williams, R.O. III, Mahaguna, V., Sriwongjanya, M.: Characterization of an inclusion complex of cholesterol and hydroxypropyl-β-cyclodextrin. Eur. J. Pharm. Biopharm. **46**(3), 355–360 (1998)
32. Pires, M.A.S., Souza dos Santos, R.A., Sinisterra, R.D.: Pharmaceutical composition of hydrochlorothiazide: β-cyclo-dextrin: Preparation by three different methods, physico-chemical characterization and in vivo diuretic activity evaluation. Molecules **16**(6), 4482–4499 (2011)
33. Klein, S., Wempe, M.F., Zoeller, T., Buchanan, N.L., Lambert, J.L., Ramsey, M.G., Edgar, K.J., Buchanan, C.M.: Improving glyburide solubility and dissolution by complexation with hydroxybutenyl-β-cyclodextrin. J. Pharm. Pharm. **61**(1), 23–30 (2009)
34. Zoeller, T., Dressman, J.B., Klein, S.: Application of a ternary HP-β-CD-complex approach to improve the dissolution performance of a poorly soluble weak acid under biorelevant conditions. Int. J. Pharm. **430**(1), 176–183 (2012)
35. Nasongkla, N., Wiedmann, A.F., Bruening, A., Beman, M., Ray, D., Bornmann, W.G., Boothman, D.A., Gao, J.: Enhancement of solubility and bioavailability of β-lapachone using cyclodextrin inclusion complexes. Pharm. Res. **20**(10), 1626–1633 (2003)
36. Eid, E.E., Abdul, A.B., Suliman, F.E.O., Sukari, M.A., Rasedee, A., Fatah, S.S.: Characterization of the inclusion complex of zerumbone with hydroxypropyl-β-cyclodextrin. Carbohydr. Polym. **83**, 1707–1714 (2011)
37. Vrečer, F., Vrbinc, M., Meden, A.: Characterization of piroxicam crystal modifications. Int. J. Pharm. **256**(1), 3–15 (2003)
38. Su, Y., Rao, S., Cai, Y., Yang, Y.: Preparation and characterization of the inclusion complex of hypocrellin A with hydroxypropyl-β-cyclodextrin. Eur. Food Res. Technol. **231**(5), 781–788 (2010)
39. Huang, Z., Tian, S., Ge, X., Zhang, J., Li, S., Li, M., Cheng, J., Zheng, H.: Complexation of chlorpropham with hydroxypropyl-β-cyclodextrin and its application in potato sprout inhibition. Carbohydr Polym. **107**, 241–246 (2014)
40. Nan, H., Ma, H., Zhang, R., Zhan, R.: Physiochemical properties of the complex of myricetin and hydroxypropyl-β-cyclodextrin. Trop. J. Pharm. Res. **13**(11), 1791–1796 (2014)
41. Liu, B., Zhu, X., Zeng, J., Zhao, J.: Preparation and physicochemical characterization of the supramolecular inclusion complex of naringin dihydrochalcone and hydroxypropyl-β-cyclodextrin. Food Res. Int. **54**(1), 691–696 (2013)
42. Liu, J., Qiu, L., Gao, J., Jin, Y.: Preparation, characterization and in vivo evaluation of formulation of baicalein with hydroxypropyl-β-cyclodextrin. Int. J. Pharm. **312**(1), 137–143 (2006)
43. Albanese, A., Tang, P.S., Chan, W.C.: The effect of nanoparticle size, shape, and surface chemistry on biological systems. Annu. Rev. Biomed. Eng. **14**, 1–16 (2012)
44. Chen, L., Mccrate, J.M., Lee, J.C., Li, H.: The role of surface charge on the uptake and biocompatibility of hydroxyapatite nanoparticles with osteoblast cells. Nanotechnology. **22**(10), 105708 (2011)
45. Al-Rawashdeh, N.A., Al-Sadeh, K.S., Al-Bitar, M.B.: Inclusion complexes of sunscreen agents with β-cyclodextrin: spectroscopic and molecular modeling studies. J. Spectrosc (2013).
46. Moriwaki, C., Costa, G., Ferracini, C., de Moraes, F., Zanin, G., Pineda, E., Matioli, G.: Enhancement of solubility of albendazole by complexation with β-cyclodextrin. Braz. J. Chem. Eng. **25**(2), 255–267 (2008)
47. Xia, S.-J., Ni, Z.-M., Xu, Q., Hu, B.-X., Hu, J.: Layered double hydroxides as supports for intercalation and sustained release of antihypertensive drugs. J. Solid State Chem. **181**(10), 2610–2619 (2008)
48. Ye, Y.-J., Wang, Y., Lou, K.-Y., Chen, Y.-Z., Chen, R., Gao, F.: The preparation, characterization, and pharmacokinetic studies

of chitosan nanoparticles loaded with paclitaxel/dimethyl-β-cyclodextrin inclusion complexes. Int. J. Nanomed. **10**, 4309 (2015)
49. Yousaf, A.M., Kim, D.W., Oh, Y.-K., Yong, C.S., Kim, J.O., Choi, H.-G.: Enhanced oral bioavailability of fenofibrate using polymeric nanoparticulated systems: physicochemical characterization and in vivo investigation. Int. J. Nanomed. **10**, 1819 (2015)
50. Ismail, A., Ahmad, B., Mohd, A., Rasedee, A., Suvitha, S., Behnam, K., Mohamed, Y., Manal-Mohamed, E., Siddig, I., Hapipah, M.: Dentatin isolated from Clausena excavata induces apoptosis in MCF-7cells through the intrinsic pathway with involvement of NF-kB signaling and G0/G1 cell cycle arrest: a bioassay-guided approach. J. Ethnopharmacol. **145**, 343–354 (2013)
51. Ucisik, M.H., Küpcü, S., Schuster, B., Sleytr, U.B.: Characterization of CurcuEmulsomes: nanoformulation for enhanced solubility and delivery of curcumin. J. Nanobiotechnol. **11**(1), 1 (2013)